Optik - International Journal for Light and Electron Optics 251 (2022) 168326

Contents lists available at ScienceDirect

Optik - International Journal for Light and Electron Optics

journal homepage: www.elsevier.com/locate/ijleo

Original Research Article

Near field diffraction of steel tape gratings illuminated with finite-size incoherent sources

Francisco Jose Torcal-Milla [a,b,*], Luis Miguel Sanchez-Brea [b]

[a] Applied Physics Department, Grupo de Tecnología Óptica Láser, Instituto de Investigación en Ingeniería de Aragón (i3A), Universidad de Zaragoza, 50009, Zaragoza, Spain

[b] Applied Optics Complutense Group, Optics Department, Universidad Complutense de Madrid, Facultad de Ciencias Físicas, Plaza de las Ciencias, 1, 28040, Madrid, Spain

ARTICLE INFO

Keywords:
Steel tape grating
Talbot effect
Optical encoder
Roughness

ABSTRACT

Steel tape gratings are diffraction gratings engraved on a steel substrate, whose slits are commonly manufactured by laser ablation. They behave as amplitude diffraction gratings, since the engraved slits act as strong scatters. Here, we extend previous works to the case of finite-size illumination sources, as they are used in applications such as optical encoders, where LEDs are commonly used as illumination sources. We obtain an analytical formulation for the near field behavior of this kind of gratings. When the light source increases its size, a decreasing in the contrast of the self-images is added to the effect of the surficial roughness. The agreement between analytical and numerical results is high, validating the obtained formulation. Besides, these results could be crucial in metrological applications in which steel tape gratings or other diffractive optical elements engraved on steel substrates are used, providing with a theoretical formalism to analyze the near field propagation of light after reflecting in them.

1. Introduction

Diffraction gratings are one the most important optical elements [1,2]. Due to its periodic modulation, diffraction gratings produce diffraction orders at the far field and self-images at the near field, which is called Talbot effect. It consists of the replication of the grating intensity pattern at periodical distances from the grating plane given by $z_T = 2np^2/\lambda$, with n integer, p the period of the grating, and λ the illumination wavelength. Talbot effect is well observed for amplitude or phase gratings illuminated by a collimated and monochromatic light beam but it has been analyzed from many points of view, [3–8].

In addition, gratings which modulate the polarization or spatial coherence of light are also found in the literature. Regarding the fabrication methods, amplitude gratings are usually manufactured by lithographic processes and phase gratings are commonly manufactured also by lithographic processes joined to acid etching, or by nanosecond or femtosecond laser ablation. Amplitude and phase gratings are usually manufactured on a glass substrate. It offers some advantages such as high flatness and transparency. On the opposite side, the main disadvantage is the fragility of the substrate, that makes it useless for applications where long gratings are required, such as large scale optical metrology or optical encoders. To solve this issue, steel tape gratings are used, [9,10]. Steel is easier to handle and allows to manufacture diffraction gratings as long as needed. Reflective amplitude or phase gratings are possible on a steel tape. To obtain phase-based diffraction gratings, femtosecond laser sources can be used, since they remove material from the surface of the steel and generate high quality grooves. On the other hand, amplitude gratings on steel tape can be obtained by lithographic processes with acid etching or by laser ablation with nanosecond laser sources.

* Corresponding author.
E-mail address: fjtorcal@unizar.es (F.J. Torcal-Milla).

https://doi.org/10.1016/j.ijleo.2021.168326
Received 16 September 2020; Received in revised form 19 October 2021; Accepted 9 November 2021
Available online 21 November 2021

In both cases, the engraved slits present roughness which acts as a strong scatter. As a consequence, the grating behaves almost as a conventional amplitude diffraction grating in reflection, [11,12]. Roughness of the steel tape which stands on the non engraved areas of the substrate produces detrimental effects such as lower contrast in higher-order self-images. A partial approach considering non constant thickness of steel substrate and its effect at the far field has been analyzed [13]. In other cases, with amplitude diffraction gratings and point source illumination or polychromatic light, the behavior is different [14]. Point-source illumination produces divergent self-images and polychromaticity of the source produces continuous fringes without the contrast inversion inherent to the Talbot effect.

In this work, the behavior of steel tape gratings at the near field is analyzed when they are illuminated by finite size illumination sources, such as LEDs. We find that the contrast of the self-images at the near field of the grating is affected by two effects: the magnitude of the roughness and the size of the source. Both effects act reducing the contrast of the self-images gradually until disappearing from a certain distance forward. These analytical results are corroborated by numerical simulations made by using a numerical integration of the Rayleigh–Sommerfeld formulation [15]. In our opinion, the formalism obtained in this work has potential applications en all optical-control systems based on self-imaging effect since it facilitates the theoretical analysis of the systems before performing the experiment or mounting the device.

2. Theoretical approach

Let us consider an one-dimensional steel tape grating whose reflectance, $S(x)$, is defined as the product of the reflectance of the rough surface, $r(x)$, and the reflectance of a conventional amplitude diffraction grating represented as a Fourier expansion, $G(x)$,

$$S(x_1) = r(x_1)G(x_1) = r(x_1)\sum_n a_n e^{iqnx_1}, \tag{1}$$

where i is the imaginary unit, a_n are the Fourier coefficients and $q = 2\pi/p$ with p the period of the grating. When the diffraction grating is illuminated by a point light source placed at a distance z_0 from the grating plane and x_0 from the optical axis, the field just after the grating can be expressed, in paraxial approximation, as

$$U(x_1) = A_0\, e^{-i\frac{k(x_1-x_0)^2}{2z_0}} S(x_1), \tag{2}$$

where $k = 2\pi/\lambda$ is the wavenumber, A_0 is the amplitude of the lightwave, and we have dropped some constant factors that will disappear after integrations. The field at a distance z from the grating is obtained by Fresnel approximation, that in 1D approach results

$$U(x_2, z) = \int U(x_1) e^{-i\frac{k(x_2-x_1)^2}{2z}} dx_1, \tag{3}$$

where the intensity is $I(x_2, z) = U(x_2, z)U^*(x_2, z)$.

Since the steel surface $r(x_1)$ is random, the surface has to be described by statistical parameters. We have assumed normal distribution in heights, $w(h) = exp\left(-h^2/2\sigma^2\right)/\sqrt{2\pi}\sigma$, where $h = h(x_1)$ and σ is the standard deviation in heights, [11,16]. Thus, the characteristic function that describes the mean reflectance of the surficial roughness is given by

$$\langle r(x_1)\rangle = \int w(h) exp\,[2ikh]\, dh = e^{-g/2}, \tag{4}$$

with $g = (2k\sigma)^2$. The relationship between two different points of the surface must be also defined. Assuming Gaussian distribution in heights with variance σ^2 and mean value zero, it results in

$$w\left[h(x_1), h(x_1')\right] = \frac{1}{2\pi\sigma\sqrt{1-C(\tau)^2}} e^{-\frac{h^2(x_1)+h^2(x_1')-2C(\tau)h(x_1)h(x_1')}{2\sigma^2\left(1-C(\tau)^2\right)}}, \tag{5}$$

where Gaussian autocorrelation coefficient is supposed,

$$C(\tau) = \frac{\langle h(x_1)h(x_1')\rangle}{\langle h^2(x_1)\rangle} = e^{-\tau^2/T_0^2}, \tag{6}$$

with $\tau = x_1 - x_1'$ and T_0 the correlation length. As a result, the characteristic function of this distribution is

$$\langle r(x_1)r(x_1')\rangle = exp^{-g[1-C(\tau)]} = e^{-g}\sum_{m=0}^{\infty}\frac{g^m}{m!}e^{-m\frac{\tau^2}{T_0^2}}. \tag{7}$$

Then, the mutual intensity function, $J(x_2, x_2', z)$, at a distance z from the grating plane results in

$$J(x_2, x_2', z) = \iint \langle U(x_1)U^*(x_1')\rangle e^{-i\frac{k(x_2-x_1)^2}{2z}} e^{i\frac{k(x_2'-x_1')^2}{2z}} dx_1 dx_1'. \tag{8}$$

Expanding all terms, the integral may be rewritten as

$$J(x_2,x_2',z) = \iint A_0^2 e^{-i\frac{k(x_1-x_0)^2}{2z_0}} e^{i\frac{k(x'_1-x_0)^2}{2z_0}} e^{-i\frac{k(x_2-x_1)^2}{2z}} e^{i\frac{k\left(x_2'-x_1'\right)^2}{2z}} \times \langle r(x_1)r(x_1')\rangle \sum_{n,n'} a_n a_{n'}^* e^{iqnx_1} e^{-iqn'x_1'} dx_1 dx_1', \tag{9}$$

where $\langle r(x_1)r(x_1')\rangle$ is given by Eq. (7). Performing both integrals and calculating the average intensity as $\langle I(x_2,z)\rangle = J(x_2,x_2,z)$, results in

$$I(x_2,z) = A_0^2 \frac{2\pi z z_0}{k(z+z_0)} e^{-g} \sum_{n,n'} a_n a_{n'}^* \sum_{m=0}^{\infty} \frac{g^m}{m!} e^{-m\left[\frac{(n-n')qzz_0}{kT_0(z+z_0)}\right]^2} e^{i\left[\frac{(n^2-n'^2)q^2zz_0}{2k(z+z_0)} + \frac{(n-n')q(x_0z+x_2z_0)}{z+z_0}\right]}, \tag{10}$$

This equation is also valid for convergent illumination just changing the sign of z_0. Some examples of diffracted mean intensity obtained using Eq. (10) are shown in Fig. 1 for several values of the standard deviation of heights and correlation lengths that cover the usual values for standard steel tape roughness. Besides, we have used different roughness values to understand how it affects to the self-imaging process. When the standard deviation of heights increases, a loss of contrast in higher order self-images is produced. On the other hand, the self-images have higher contrast when the roughness is smaller

From Eq. (10), we may obtain the intensity for monochromatic, plane wave illumination by applying $z_0 \to \infty$. Then the intensity results in

$$I_{PW}(x_2,z) = A_0^2 \frac{2\pi z}{k} e^{-g} \sum_{n,n'} a_n a_{n'}^* \sum_{m=0}^{\infty} \frac{g^m}{m!} e^{-m\left[\frac{(n-n')qz}{kT_0}\right]^2} e^{i\left[\frac{(n^2-n'^2)q^2z}{2k} + (n-n')qx_2\right]}, \tag{11}$$

which is obtained in [12] but considering higher orders to describe the surficial roughness.

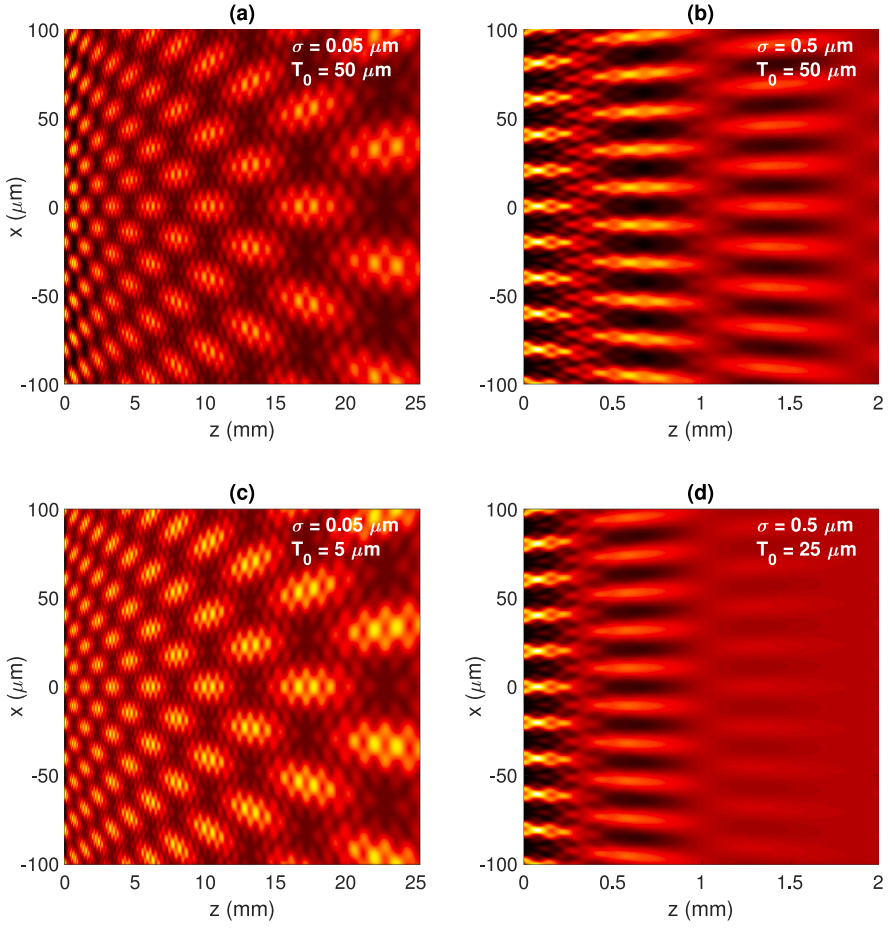

Fig. 1. Average intensity computed with Eq. (10) (point source illumination), $\lambda = 632.8$ nm, $p = 20$ μm, $n = n' = (-10,-9,\ldots,9,10)$, $m = 0,1$, $z_0 = 10$ mm, for different values of T_0 and σ.

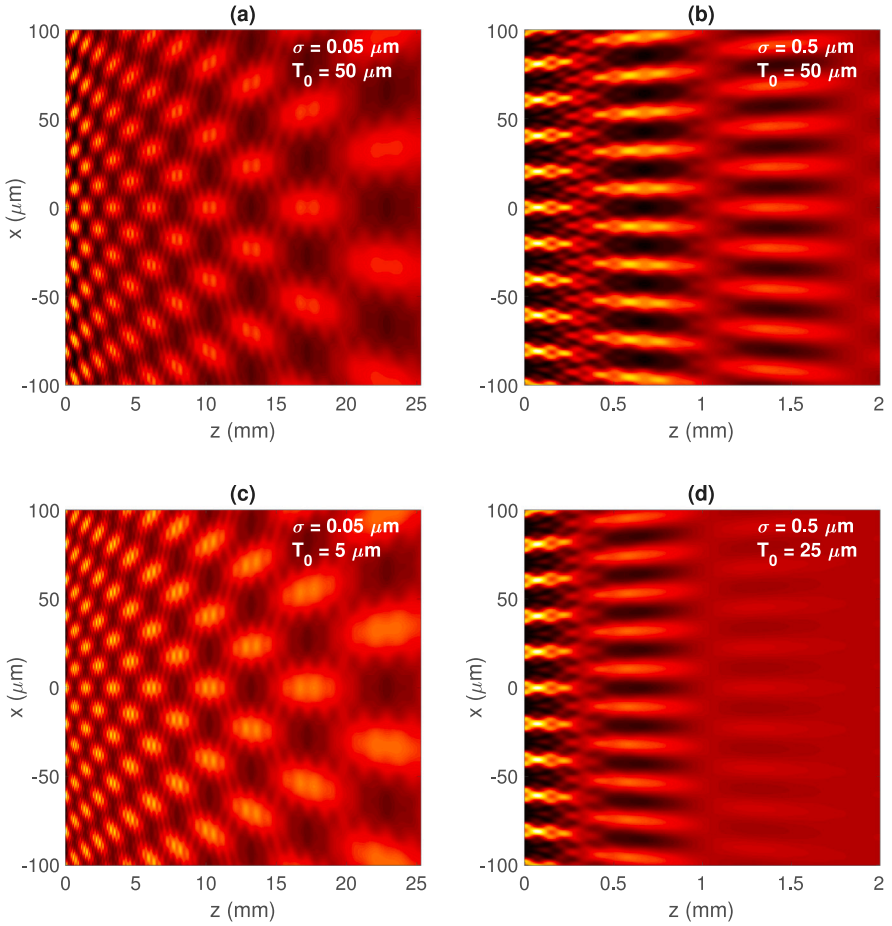

Fig. 2. Average intensity computed with Eq. (14) (finite-size illumination), $\lambda = 632.8$ nm, $p = 20$ μm, $n = n' = (-10, -9, \ldots, 9, 10)$, $m = 0, 1$, $z_0 = 10$ mm, $L = 10$ μm, for different values of T_0 and σ.

Also, when no roughness is present, $T_0 \to \infty$ and $\sigma = 0$, the intensity is

$$I_{NR}(x_2, z) = A_0^2 \frac{2\pi z z_0}{k(z+z_0)} \sum_{n,n'} a_n a_{n'}^* e^{i\left[\frac{(n^2-n'^2)q^2 z z_0}{2k(z+z_0)} + \frac{(n-n')q(x_0 z + x_2 z_0)}{z+z_0}\right]}, \tag{12}$$

which is obtained in [14]. Both limit results corroborate partially the validity of the present formalism.

Now, let us analyze the effect of the finite size of the light source. An integration over x_0 is required, since this parameter is the position of the light source along the axis parallel to the diffraction grating. Thus, the intensity is obtained by

$$\begin{aligned} I_{FS}(x_2, z) = {} & A_0^2 \frac{2\pi z z_0}{k(z+z_0)} e^{-g} \sum_{n,n'} a_n a_{n'}^* \sum_{m=0}^{\infty} \frac{g^m}{m!} e^{-m\left[\frac{(n-n')qzz_0}{kT_0(z+z_0)}\right]^2} \\ & \times e^{i\left[\frac{(n^2-n'^2)q^2 z z_0}{2k(z+z_0)} + \frac{(n-n')qx_2 z_0}{z+z_0}\right]} \int_{-L/2}^{+L/2} e^{i\left[\frac{(n-n')qz}{z+z_0} x_0\right]} dx_0, \end{aligned} \tag{13}$$

where L is source size, which is centered at the optical axis. The intensity results

$$\begin{aligned} I_{FS}(x_2, z) \propto {} & e^{-g} \sum_{n,n'} a_n a_{n'}^* \sum_{m=0}^{\infty} \frac{g^m}{m!} e^{-m\left[\frac{(n-n')qzz_0}{kT_0(z+z_0)}\right]^2} \\ & \times e^{i\left[\frac{(n^2-n'^2)q^2 z z_0}{2k(z+z_0)} + \frac{(n-n')qx_2 z_0}{z+z_0}\right]} sinc\left[\frac{(n-n')qzL}{2(z+z_0)}\right]. \end{aligned} \tag{14}$$

We show in Fig. 2 the same examples than in Fig. 1 but considering a finite size monochromatic light source with lateral size $L = 10$ μm instead of point source illumination. The size of the source has been chosen small enough to produce self-images and big

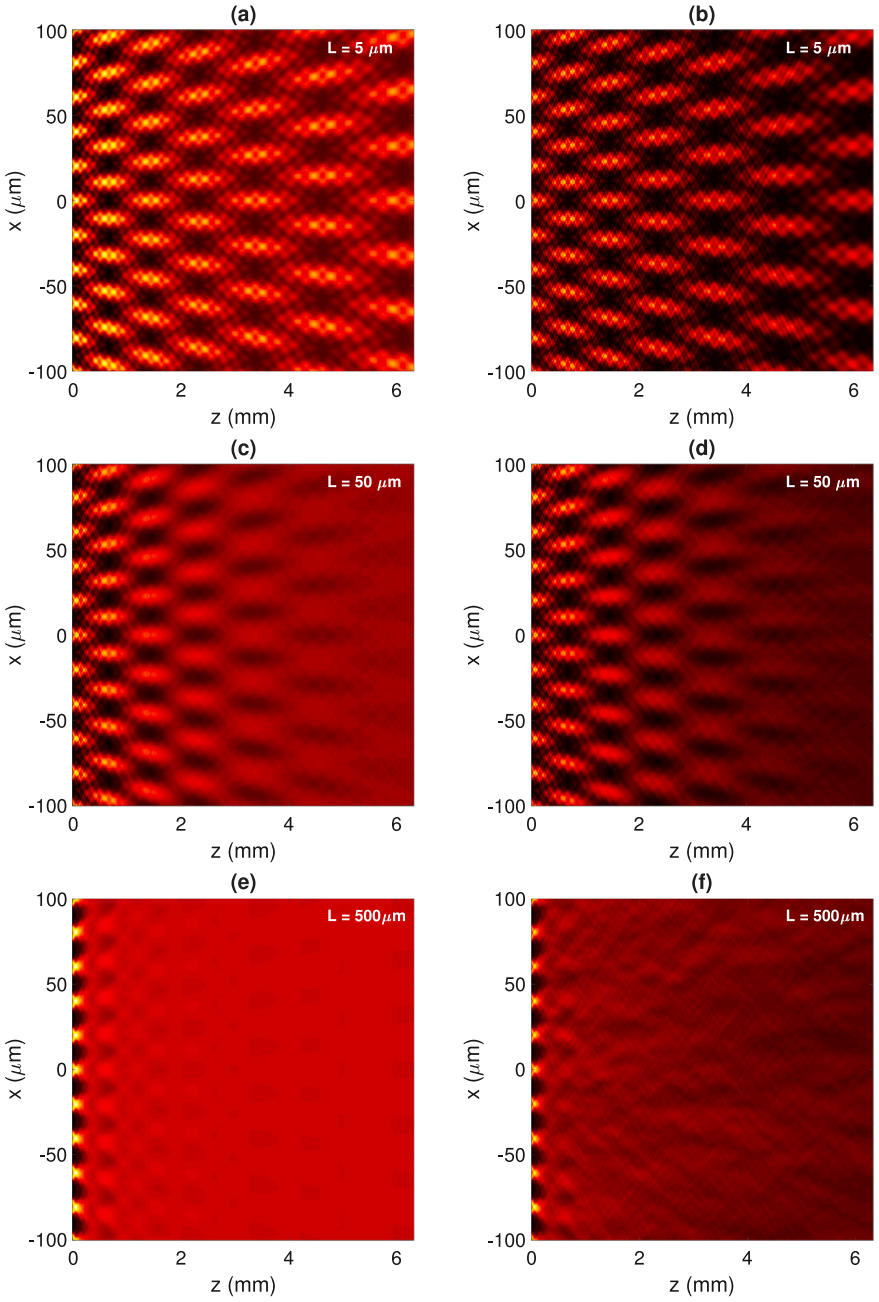

Fig. 3. (a, c, and e) average intensity computed with Eq. (14), $n = n' = (-3, -2, \ldots, 2, 3)$, (b, d, and f) average intensity computed numerically over 100 realizations. $\lambda = 632.8$ nm, $p = 20$ μm, $m = 0, 1$, $z_0 = 10$ mm, $\sigma = 0.05$ μm, and $T_0 = 50$ μm. The size of the source is written into each subfigure.

enough to produce decreasing of contrast for high self-images. In addition, there are in the market several LEDs with size around the selected value [17]. Comparing Fig. 2(a) and (c) with Fig. 1(a) and (c), a blurring of higher order self-images due to the finite size of the light source is observed. However, this effect is not observed in Fig. 2(b) and (d), compared to Fig. 1(b) and (d), since higher self-images do not exist due to the surficial roughness of the steel tape.

Also, the dependence of the near field diffraction pattern on the size of the source for the same roughness parameters is shown in Fig. 3(a), (c), and (e). When the light source size is increased, the contrast of the self-images at the near field decreases. So, the larger is the source, the lesser is the number of self-images with measurable contrast. Finally, only zeroth order self-image remains from a certain source size forward.

3. Numerical simulations

To corroborate the theoretical formalism, we have numerically simulated the steel tape diffraction gratings and obtained the near field diffraction pattern of this gratings using Diffractio package [15]. An example of the reflectance of a steel tape grating is shown in Fig. 4, which is obtained by multiplying the reflectance of a common amplitude Ronchi grating and the topography of the steel tape. The reflection coefficient can be obtained from the topography as $R(x_1) = exp[2ik\ S(x_1)]$. The analytical formalism implies an average which, in practical applications, is given by the two-dimensionality of the grating. Each row of the grating acts as an one-dimensional grating but the diffracted field is composed by the incoherent summation of all of them. One realization corresponding to the same gratings used to obtain Fig. 2 is shown in Fig. 5. For just one realization, the diffraction pattern is not homogeneous. This is more evident for longer correlation length of roughness. To compare the numerical results to that obtained analytically, we show in Fig. 6 the numerical average over 100 random realizations, corresponding to each case of Fig. 5. The results are very similar to those obtained in Fig. 2. Besides, we may observe in Fig. 3(b), (d), and (f) the numerical simulations corresponding to the same gratings computed analytically, Fig. 3(a), (c), and (e), in which we have varied the size of the source remaining the amount of roughness as a constant. The agreement between analytical and numerical results is clear, validating the obtained formalism. Although the numerical simulations corroborate the analytical formalism, an experiment could be proposed. The experiment would be similar to those performed in [14,18]. It consists on a reflection configuration set-up by using a beam splitter. The light is taken by a CCD sensor which is displaced parallel to the optical axis and the images are vertically integrated to obtain the mean intensity at each perpendicular plane. The obtained images would be similar to those shown in Figs. 2 and 6. The illumination source for the experiment should be as small as possible, so we would recommend the usage of a VCSEL or a microLED, [17].

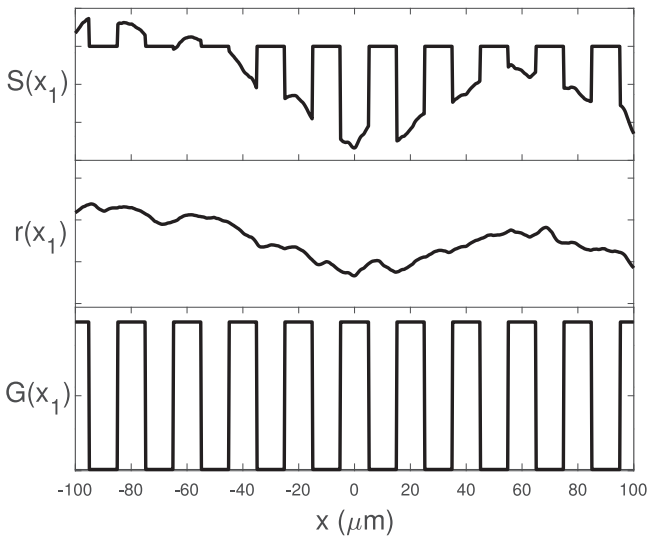

Fig. 4. Example of the reflectance for one realization of steel tape grating, used for the numerical simulations. The parameters of the grating are $p = 20$ μm, $\sigma = 0.05$ μm, $T_0 = 25$ μm. $G(x_1)$ is the reflectance of a common amplitude Ronchi grating, $r(x_1)$ is the topography of the steel tape, and $S(x_1)$ is the reflectance of the topography of the steel tape grating.

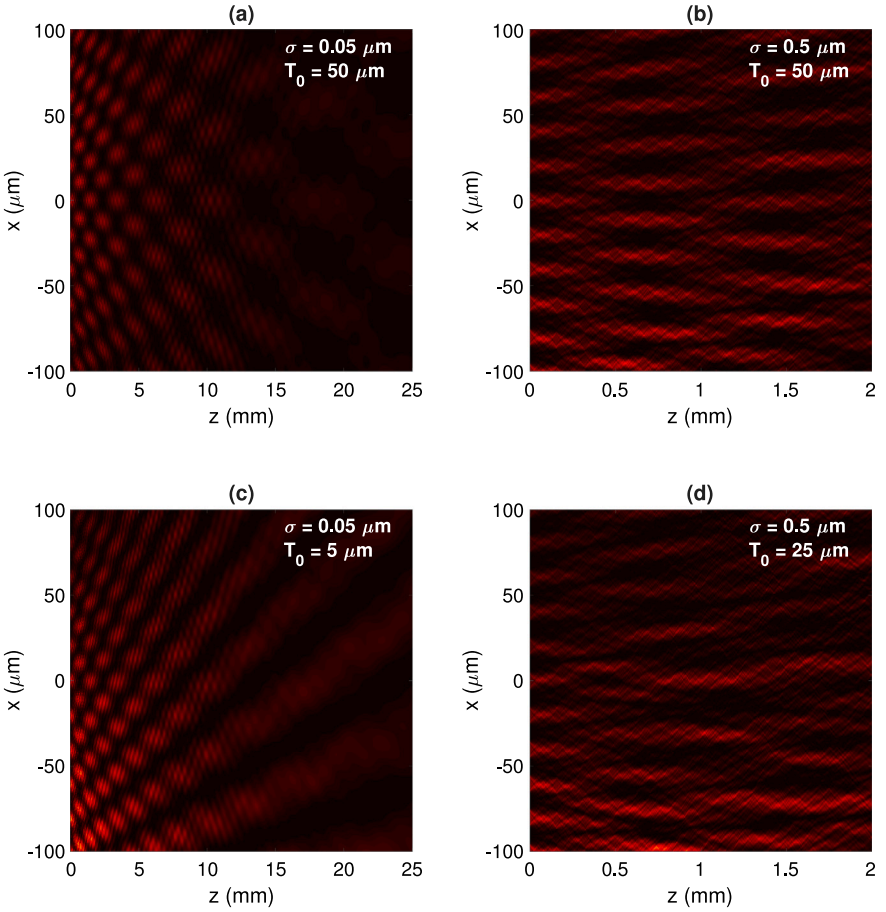

Fig. 5. Intensity computed numerically for one realization (finite-size illumination), $\lambda = 632.8$ nm, $p = 20$ μm, $z_0 = 10$ mm, $L = 10$ μm, for different values of T_0 and σ.

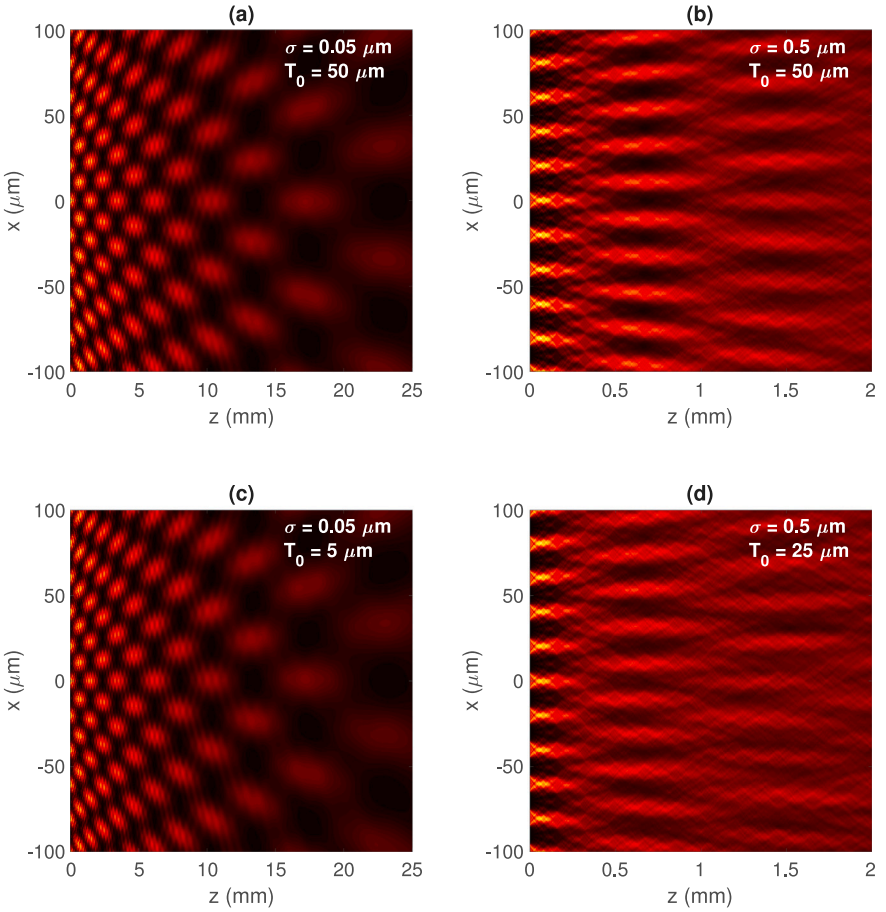

Fig. 6. Average intensity computed numerically from 100 realizations (finite-size illumination), $\lambda = 632.8$ nm, $p = 20$ μm, $z_0 = 10$ mm, $L = 10$ μm, for different values of T_0 and σ.

Conclusions

The near field behavior of steel tape gratings illuminated by incoherent finite-size light sources, such as a LED, is analyzed. We obtain the expressions for the near field intensity in terms of the roughness parameters of the steel tape, and the parameters of the source and grating. We find that the contrast of the self-images at the near field is a combination of two effects: the magnitude of the roughness and the finite size of the source. Both effects reduce the contrast of the self-images. Numerical simulations are performed, which highly agree to analytical results. The obtained formalism is important in applications in which self-images are used for metrology, such as optical encoders and allows to theoretically analyze the system before performing experiments or manufacturing a device.

Declaration of competing interest

The authors declare that they have no known competing financial interests or personal relationships that could have appeared to influence the work reported in this paper.

Acknowledgments

Dr. Torcal-Milla acknowledges support by Gobierno de Aragón-Fondo Social Europeo (Grupo de Tecnología Óptica Láser-E44_20R). Dr. Sanchez-Brea acknowledges funding from Ministerio de Ciencia e Innovación: Retos Colaboración 2019, Teluro project RTC2019-007113-3, and from Plan Nacional de Investigación, Nanorooms project PID2019- 105918GB-I00.

References

[1] C.A. Palmer, E.G. Loewen, Diffraction Grating Handbook, Newport Corporation New York, 2005.
[2] E.G. Loewen, E. Popov, Diffraction Gratings and Applications, CRC Press, 2018.
[3] Y. Zhang, Z. Wang, Z. Nie, C. Li, H. Chen, K. Lu, M. Xiao, Four-wave mixing dipole soliton in laser-induced atomic gratings, Phys. Rev. Lett. 106 (9) (2011) 093904.
[4] Z. Zhang, X. Liu, D. Zhang, J. Sheng, Y. Zhang, Y. Zhang, M. Xiao, Observation of electromagnetically induced Talbot effect in an atomic system, Phys. Rev. A 97 (1) (2018) 013603.
[5] Z. Zhang, L. Yang, J. Feng, J. Sheng, Y. Zhang, Y. Zhang, M. Xiao, Parity-time-symmetric optical lattice with alternating gain and loss atomic configurations, Laser Photonics Rev. 12 (10) (2018) 1800155.
[6] L.A. Hall, M. Yessenov, S.A. Ponomarenko, A.F. Abouraddy, The space–time Talbot effect, APL Photon. 6 (5) (2021) 056105.
[7] L. Li, H. Liu, X. Chen, Dynamic manipulation of nonlinear Talbot effect with structured light, Opt. Lett. 46 (6) (2021) 1281–1284.
[8] M. Yessenov, L.A. Hall, S.A. Ponomarenko, A.F. Abouraddy, Veiled talbot effect, Phys. Rev. Lett. 125 (24) (2020) 243901.
[9] F.J. Salgado-Remacha, L.M. Sanchez-Brea, F.J. Alvarez-Rios, E. Bernabeu, Rough Fresnel zone plates over metallic surfaces, Appl. Opt. 49 (10) (2010) 1750–1756.
[10] F.J. Salgado-Remacha, F.J. Torcal-Milla, L.M. Sanchez-Brea, E. Bernabeu, Use of steel substrates in diffractive optics: near field of high surface quality steel tape gratings, Opt. Lasers Eng. 49 (3) (2011) 356–360.
[11] J.A. Ogilvy, Theory of Wave Scattering from Random Rough Surfaces, CRC Press, 1991.
[12] F.J. Torcal-Milla, L.M. Sanchez-Brea, E. Bernabeu, Talbot effect with rough reflection gratings, Appl. Opt. 46 (18) (2007) 3668–3673.
[13] X. Mi, S. Zhang, X. Qi, H. Yu, J. Zhou, S. Jiang, Effect of thickness non-uniformity of large-area grating metal film on grating diffraction wavefront, Opt. Laser Technol. 119 (2019) 105675.
[14] F.J. Torcal-Milla, L.M. Sanchez-Brea, Achromatic self-imaging with finite extension light sources, J. Opt. 17 (12) (2015) 125605.
[15] L.M. Sanchez-Brea, Diffractio, python module for diffraction and interference optics, 2019.
[16] P. Beckmann, A. Spizzichino, The Scattering of Electromagnetic Waves from Rough Surfaces, Artech House, Inc., Norwood, MA, 1987, 511 P..
[17] P.J. Parbrook, B. Corbett, J. Han, T.-Y. Seong, H. Amano, Micro-light emitting diode: From chips to applications, Laser Photonics Rev. 15 (5) (2021) 2000133.
[18] F.J. Torcal-Milla, L.M. Sanchez-Brea, E. Bernabeu, Self-imaging of gratings with rough strips, J. Opt. Soc. Amer. A 25 (10) (2008) 2390–2394.